Available online at www.sciencedirect.com

SCIENCE DIRECT

Biochimica et Biophysica Acta 1715 (2005) 104 – 110

BIOCHIMICA ET BIOPHYSICA ACTA

BBA

http://www.elsevier.com/locate/bba

Site-directed mutagenesis of cysteine residues of large neutral amino acid transporter LAT1

Ruben J. Boado*, Jian Yi Li [1], Chun Chu, Fumio Ogoshi, Petra Wise, William M. Pardridge

Department of Medicine, UCLA Warren Hall 13-164, 900 Veteran Ave., Los Angeles, CA 90024, USA

Received 4 May 2005; received in revised form 16 July 2005; accepted 20 July 2005
Available online 2 August 2005

Abstract

The large neutral amino acid transporter type 1, LAT1, is the principal neutral amino acid transporter expressed at the blood–brain barrier (BBB). Owing to the high affinity (low K_m) of the LAT1 isoform, BBB amino acid transport in vivo is very sensitive to transport competition effects induced by hyperaminoacidemias, such as phenylketonuria. The low K_m of LAT1 is a function of specific amino acid residues, and the transporter is comprised of 12 phylogenetically conserved cysteine (Cys) residues. LAT1 is highly sensitive to inhibition by inorganic mercury, but the specific cysteine residue(s) of LAT1 that account for the mercury sensitivity is not known. LAT1 forms a heterodimer with the 4F2hc heavy chain, which are joined by a disulfide bond between Cys^{160} of LAT1 and Cys^{110} of 4F2hc. The present studies use site-directed mutagenesis to convert each of the 12 cysteines of LAT1 and each of the 2 cysteines of 4F2hc into serine residues. Mutation of the cysteine residues of the 4F2hc heavy chain of the hetero-dimeric transporter did not affect transporter activity. The wild type LAT1 was inhibited by $HgCl_2$ with a K_i of 0.56 ± 0.11 μM. The inhibitory effect of $HgCl_2$ for all 12 LAT1 Cys mutants was examined. However, except for the C439S mutant, the inhibition by $HgCl_2$ for 11 of the 12 Cys mutants was comparable to the wild type transporter. Mutation of only 2 of the 12 cysteine residues of the LAT1 light chain, Cys^{88} and Cys^{439}, altered amino acid transport. The V_{max} was decreased 50% for the C88S mutant. A kinetic analysis of the C439S mutant could not be performed because transporter activity was not significantly above background. Confocal microscopy showed the C439S LAT1 mutant was not effectively transferred to the oocyte plasma membrane. These studies show that the Cys^{439} residue of LAT1 plays a significant role in either folding or insertion of the transporter protein in the plasma membrane.

Keywords: Phenylketonuria; PKU; Brain amino acid transport; LAT1; Site-directed mutagenesis

1. Introduction

Hyperaminoacidemias such as phenylketonuria (PKU) selectively impair amino acid metabolism in the central nervous system (CNS), owing to the very high affinity (low K_m) of the blood–brain barrier (BBB) amino acid transporter [1]. The transport of large neutral amino acids (LNAA) such as phenylalanine across the BBB is mediated by the LAT1 isoform [2], which is a member of the Solute Carrier (SLC)-7 gene family, and was originally cloned from rat glial tumor cells [3]. BBB LAT1 is normally 90% saturated by circulating LNAAs [1]. Consequently, when the plasma concentration of a specific LNAA, e.g., phenylalanine, is selectively elevated, the brain uptake of the other LNAAs is impaired because the BBB LAT1 transporter is saturated. The high affinity (low K_m) of the BBB LAT1 transporter is a function of the specific amino acids comprising the active site on the transporter. A prominent feature of the LAT1 structure is the phylogenetic conservation of all 12 cysteine (Cys) residues [4]. The LAT1 polypeptide inserts in the plasma membrane as a heterodimer with the 4F2hc heavy chain, and these two subunits are joined by a disulfide bond between Cys^{160} of LAT1 and Cys^{110} of 4F2hc [5]. However, site-directed mutagenesis of these cysteine residues on either LAT1 or 4F2hc does not

* Corresponding author. Tel.: +1 310 825 8858; fax: +1 310 206 5163.
E-mail address: rboado@mednet.ucla.edu (R.J. Boado).
[1] Present address: Department of Pathology, University of Oklahoma, Oklahoma City, OK.

0005-2736/$ - see front matter © 2005 Elsevier B.V. All rights reserved.
doi:10.1016/j.bbamem.2005.07.007

inhibit amino acid transport and does not eliminate the high sensitivity of this transporter to inorganic mercury [6]. Therefore, the purpose of the present study was to perform a systematic mutagenesis of each of these 14 cysteine residues of the LAT1 light chain or the 4F2hc heavy chain. The cloned RNA is injected in frog oocytes followed by measurements of the kinetics of phenylalanine transport.

2. Materials and methods

2.1. Materials

[^{14}C]-sucrose (0.6 Ci/mmol) was purchased from Perkin Elmer Life Science (Boston, MA). [^{3}H]-phenylalanine (26 Ci/mmol) was obtained from Amersham Pharmacia Biotech (Arlington, IL). The mMessage mMachine™ in vitro transcription kit was obtained from Ambion (Austin, TX). *Not*I was obtained from New England Biolabs (Beverly, MA). All other restriction endonucleases were obtained from Promega Life Science (Madison, WI). The QuickChange site-directed mutagenesis kit and *E. coli* XL1 blue supercompetent cells were obtained from Stratagene (San Diego, CA). Plasmid isolation kits were purchased form Qiagen (Valencia, CA). Female oocyte-positive *Xenopus laevis* (50–70 g) were purchased from Nasco (Fort Atkinson, WI). Phenylalanine, mercuric chloride and other molecular biology grade reagents were obtained from Sigma-Aldrich Chemicals (St. Louis, MI). Oligodeoxynucleotides were custom synthesized at Biosource International (Camarillo, CA). The Quick Start Mix and other DNA sequencing-related reagents were obtained from Beckman-Coulter (Fullerton, CA). The rabbit LAT1 and 4F2hc cDNAs (accession # AF515772 and AF515773, respectively) were prepared in this laboratory as previously described [4]. Alexafluor-488 conjugated to goat-anti-rabbit immunoglobulin G (IgG) was purchased from Molecular Probes (Eugene, OR).

2.2. Site-directed mutagenesis (SDM)

SDM of Cys residues of either the rabbit 4F2hc heavy chain or the rabbit LAT1 light chain (Table 1) was performed using the QuickChange SDM kit as previously reported in this laboratory [4]. Forward and reverse SDM primers containing the desired mutation and 15 nucleotides of both 5′- and 3′-flanking region of the sequence were designed to anneal on opposite strands of plasmid DNA and had a T_m > 78 °C. SDM reactions were performed with 100 ng plasmid DNA, 125 ng of each forward and reverse primer, dNTPs, 7% dimethylsulfoxide and 2.5 U Pfu Turbo DNA polymerase in a total volume of 50 μl reaction buffer. Mutated DNA was synthesized in a temperature cycler (BioRad iCycler, Hercules, CA) using a denaturing cycle of 30 s at 95 °C followed by 17 amplification cycles of 30 s at 95 °C, 1 min at 55 °C, and 16 min at 68 °C. Parental non-mutated plasmid DNA was digested with 10 U *Dpn*I for 1 h at 37 °C. XL1 blue supercompetent cells were transformed and plasmid DNA was isolated from random colonies using the Qiagen mini-prep isolation kit. The mutation rate ranged from 60 to 100%.

Table 1
Oligodeoxynucleotides (ODN) for site-directed mutagenesis

Mutation	ODN
Rabbit LAT1	
C88S	GTG GTG TGG GCC GTG TCC GGC GTC TTC TCC ATC
C98S	ATC GTG GGC GCG CTC TCC TAC GCC GAG CTG GGC
C160S	CCC GTC TTC CCC ACC AGC CCG GTG CCC GAG GAG
C172S	GCC AAG CTC GTG GCC AGC CTC TGC GTG CTG CTG
C174S	CTC GTG GCC TGC CTC AGC GTG CTG CTG CTC ACG
C183S	CTC ACG GCC GTG AAC AGC TAC AGC GTG AAG GCT
C331S	TTC GTG GGC CTG TCC AGC TTC GGT TCT GTC AAC
C377S	TCG CTC GTG TTC ACG AGC GCC ATG ACC CTG CTG
C403S	TTC TTC AAC TGG CTC AGC GTG GCC CTG GCC ATC
C439S	TTC TTC ATC CTG GCC AGC CTC TTC CTC ATC GCC
C454S	AAG ACG CCC GTG GAG AGC GGC ATC GGC TTC ACC
C492S	TCG GCC ACG GCC CTC AGT CAG AAG CTG ATG CAG
Rabbit 4F2hc	
C110S	GTG CGG GCG CCG CGC AGC CGC GAG CTG CCG GTG
C332S	ACT GAC AGT CAC TGG AGC AGC TGG AGT TTG TCG

The Cys of rabbit LAT1 or 4F2hc was converted to Ser with a single nucleotide G→C or T→A substitution (underlined).

2.3. DNA sequencing

Confirmation of each SDM was performed by DNA sequencing of the isolated clones as previously described [4]. Sequencing reactions were conducted using either the T7 or customized primers and the Quick Start Mix in a Beckman-Coulter CEQ 2000XL DNA sequencer. Samples were resolved as per the manufacturer's instructions with the following running conditions: capillary temperature, 50 °C; denaturation, 120 s at 90 °C; injection, 15 s at 2 kV; separation, 85 min at 4.2 kV.

2.4. In vitro transcription (IVT) and expression in oocytes

In vitro transcription was performed with pSPORT vectors encoding the wild type or mutated rabbit LAT1 and 4F2hc cDNAs linearized with *Not*I [4]. Synthesis of cloned RNA (cRNA) was completed in the presence of T7 RNA polymerase and 5′-capped analog using the mMessage mMachine kit. The length of the various capped cRNAs was confirmed by denaturing gel electrophoresis and ethidium bromide staining. Frog oocytes were isolated as described previously [7] and injected with 50 nl of water or cRNA solution (10–30 ng/oocyte) using a nanoliter injector (World Precision Instruments, Sarasota, FL) [2]. Oocytes were incubated in Barth's/gentamycin solution for 3 days at 18 °C to allow for expression of the various mRNA. LAT1 transport activity was assayed in 8 to 10 oocytes using 150 μl of sodium buffer (0.1 M NaCl,

2 mM KCl, 1 mM $MgCl_2$ 1 mM $CaCl_2$, 10 mM HEPES, pH 7.5) containing 0.6 μCi of [^{3}H]-phenylalanine and 0.048 μCi of [^{14}C]-sucrose without or with unlabeled phenylalanine for 3 min at 22 °C. For the $HgCl_2$ inhibition experiments, oocytes were pre-incubated in the presence of the specific concentration of $HgCl_2$ for 15 min at 23 °C, followed by addition of [^{3}H]-phenylalanine and [^{14}C]-sucrose; the uptake incubation was terminated 3 min later. The reaction was stopped with 4 ml of ice-cold sodium buffer, followed by 3 additional washes with sodium buffer. Oocytes were individually dissolved in 0.5 ml of 1 M NaOH for 30 min at 60 °C. The radioactivity was measured in a liquid scintillation counter (Packard TRI-CARB 2100TR, Meriden, CT) with windows for dual isotope counting (i.e. ^{3}H, ^{14}C). The phenylalanine and sucrose volumes of distribution (VD), μl per oocyte, were calculated as follows: VD=(DPM per oocyte)/(DPM per μl medium), and the sucrose VD was subtracted from the phenylalanine VD. The corrected phenylalanine VD was divided by the incubation time (3 min) to give the clearance in nL/oocyte/min.

2.5. Kinetic analysis

The kinetic parameters of phenylalanine clearance (Cl) by the oocyte were determined by fitting the clearance data to the Michaelis–Menten equation $Cl=[V_{max}/(K_m+S)]+K_D$, where S=the medium phenylalanine concentration, and the following parameters were calculated: the maximal transport rate (V_{max}), the half-saturation constant (K_m), and the constant of non-saturable transport (K_D). For computation of the $HgCl_2$ K_i, the phenylalanine clearance was fit to: $Cl=(V_{max}/K_m)[K_i/(K_i+I)]+K_D$, where I=the $HgCl_2$ concentration, K_i is the $HgCl_2$ half-inhibition constant, and the V_{max}/K_m ratio and K_D are parameters of [^{3}H]-phenylalanine transport. In the K_i kinetic analysis, 3 parameters were estimated: the $HgCl_2$ K_i, the phenylalanine (V_{max}/K_m) ratio, and the phenylalanine K_D. Data fits were determined by nonlinear regression analysis using program P3R from the BMDP Statistical Software developed by the University of California Los Angeles BMDP Computing Facility as previously described [8]. Statistical analysis was performed with analysis of variance (ANOVA) with Bonferroni correction using program 7D of the BMDP Statistical Software package, and a P value <0.05 was considered statistically significant.

2.6. LAT1 antibody production

A synthetic peptide corresponding to the 15 amino acids of the amino terminus of bovine LAT1, plus a carboxy terminal cysteine, was synthesized by Multiple Peptide Systems (San Diego, CA). The amino acid sequence of bovine and rabbit LAT1 are conserved with 3 conservative substitutions [4]. The LAT1 amino terminal peptide was conjugated at the cysteine residue to bovine thyroglobulin with m-maleimidobenzoyl-N-hydroxysuccinimide ester for immunization of adult New Zealand rabbits with Hunter's Titer-Max as the adjuvant. The antisera titers were determined with an ELISA using the synthetic peptide as antigen. For affinity purification of the anti-LAT1 antibodies, 2.0 mg of synthetic peptide was conjugated to 1.0 g of cyanogen bromide activated Sepharose 4 Fast Flow. The rabbit anti-LAT1 antiserum (4.0 ml) was applied to the column equilibrated in 0.01 M Tris, 0.15 M NaCl, pH=7.8, 1 mM EDTA, followed by elution of non-specific protein with 0.1 M Na acetate, 0.5 M NaCl, pH=4.0. The anti-LAT1 antibodies were eluted with 0.1 M acetic acid, followed by neutralization to pH=7 with 1 M NH_4OH.

2.7. Confocal microscopy of oocytes

Cloned RNA (cRNA) corresponding to either wild type rabbit LAT1 or the C439S mutant, or water, was injected with 4F2hc into frog oocytes as described above, followed by incubation at 18 °C for 3 days. The oocytes were placed in a cryomold, covered with Tissue Tek O.C.T. embedding compound and rapidly frozen in powdered dry ice. Frozen sections, 8 μm, were prepared on a Mikron HM505E cryostat, followed by fixation in 100% acetone at −20 °C for 5 min. The sections were incubated with affinity purified anti-LAT1 antibodies or rabbit IgG negative control, 10 μg/ml, overnight at 4 °C, followed by immune labeling with Alexafluor-488-conjugated goat anti-rabbit IgG for 60 min at room temperature. Sections were cover-slipped and viewed under a 20× objective in single-track mode with a Zeiss LSM 5 PASCAL confocal microscope with dual argon and helium/neon lasers.

3. Results

The conversion of either Cys^{110} or Cys^{332} of the rabbit 4F2hc heavy chain causes no inhibition of phenylalanine transport in frog oocytes (Fig. 1). The individual conversion of the 12 cysteine residues in the LAT1 light chain to serine residues identifies only two sites, Cys^{88} and Cys^{439} that results in a decrease in phenylalanine transport by the mutated transporter (Fig. 1). Phenylalanine saturation curves were performed on more than half of these mutants. The phenylalanine saturation curve for the wild type (wt) and the C439S mutant is shown in Fig. 2 and the Michaelis–Menten kinetic parameters for transport via the wild type transporter are shown in Table 2. The kinetic parameters for the C439S mutant were not computed because the clearance of phenylalanine by the oocytes co-injected with wild type 4F2hc and C439S mutant cRNA was not higher than the phenylalanine clearance in oocytes injected with wild type 4F2hc cRNA alone (Fig. 3). The V_{max} of phenylalanine transport is decreased 50% for the C88S LAT1 mutant; however, the V_{max} of phenylalanine transport is normalized for the C88S/C183S double mutant (Table 2). There is no

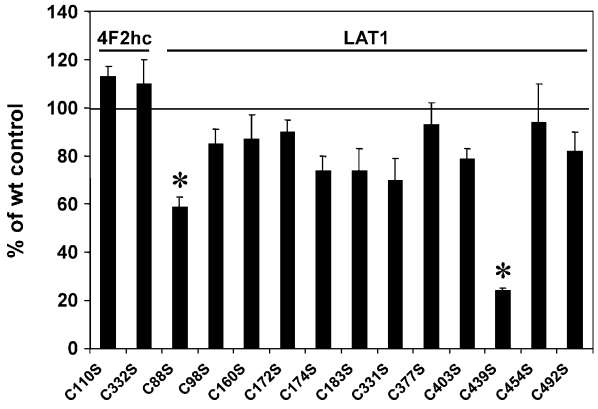

Fig. 1. The transport of [^{3}H]-phenylalanine into frog oocytes was measured at 3 days after the injection of cloned RNA expressing the wild type 4F2hc heavy chain and the LAT1 light chain. Each of the 2 cysteine residues of the 4F2hc and the 12 cysteines of the LAT1 were individually mutated to serine residues, and transporter activity of each mutant was measured relative to the wild type (wt) control shown as the horizontal solid line. Data are mean±S.E. (n=6 oocytes per measurement). The asterisk (*) indicates a significant difference from the wild type control by ANOVA with Bonferroni correction. The data were not corrected for the endogenous oocyte uptake of phenylalanine.

significant change in the K_m or V_{max} of phenylalanine transport via the C183S, the C331S, the C98S, the C492S, or the C454S LAT1 mutants, or the C98S/C183S double cysteine mutant (Table 2).

Inorganic mercury inhibited phenylalanine transport via the wild type LAT1 (Fig. 3A). Kinetic analysis of the inhibition data indicated the $HgCl_2$ K_i was 0.56±0.11 μM (Table 3). The rate of phenylalanine transport following the co-injection of wild type rabbit 4F2hc and C439S LAT1 RNA was reduced compared to amino acid transport following the injection of wild type rabbit 4F2hc RNA alone, except at very high [$HgCl_2$] (Fig. 3B). All 12 Cys mutants of LAT1 were tested for sensitivity to $HgCl_2$

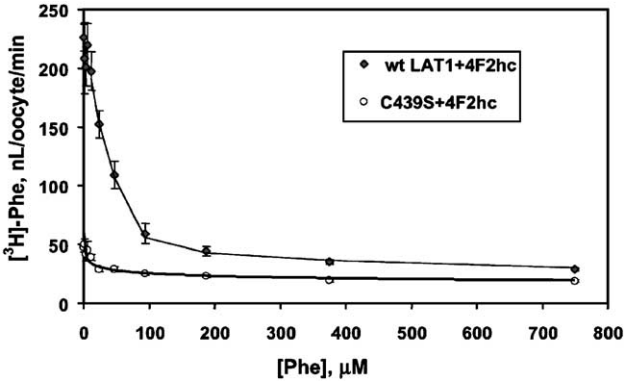

Fig. 2. The clearance (nL/oocyte/min) of [^{3}H]-phenylalanine by frog oocytes was measured in the presence of increasing concentrations of unlabeled phenylalanine (Phe). The oocytes were injected with cloned RNA encoding either wild type (wt) rabbit LAT1 and rabbit 4F2hc or the C439S mutant of rabbit LAT1 and the wt rabbit 4F2hc. Data are mean±S.E. (n=6 oocytes at each concentration of phenylalanine). The data were not corrected for the endogenous oocyte uptake of phenylalanine.

Table 2
[^{3}H]-Phenylalanine transport in frog oocytes injected with rabbit LAT1 cRNA

LAT1 variant	K_m (μM)	V_{max} (pmol/oocyte/min)	K_D (nL/oocyte/min)
Wt	19.8±3.2	6.59±0.84	20±3
C88S	16.4±2.1	3.31±0.33*	17±2
C98S	18.7±1.8	5.26±0.38	15±1
C183S	16.4±2.0	5.87±0.51	14±1
C331S	39.9±16.6	6.79±2.32	10±4
C454S	31.8±7.9	5.08±1.11	23±4
C492S	30.1±12.3	5.95±2.14	12±6
C88S/C183S	16.7±2.3	4.98±0.52	16±2
C98S/C183S	19.1±3.8	5.18±0.80	16±3

Mean±S.E., determined by non-linear regression analysis.
Differences in K_m and V_{max} values were determined by ANOVA.
* P<0.005, relative the wild type (wt) rabbit LAT1.

inhibition, as shown in Table 3 and Fig. 4. In the case of 11 out of the 12 Cys LAT1 mutants, the inhibitory effect of the $HgCl_2$ was not significantly different from the inhibitory effect of $HgCl_2$ on wild type LAT1 (Table 3, Fig. 4).

The V_{max} of phenylalanine transport via the C439S mutant was decreased >90% compared to the wild type control (Figs. 2 and 3), which suggested that the mutation of Cys^{439} may impair the ability of the transporter to insert in the oocyte membrane. Therefore, confocal microscopy was performed with affinity purified anti-LAT1 antibodies (Materials and methods). The wild type LAT1 inserted into the plasma membrane of the cRNA-injected oocyte (Fig. 5A). In contrast, no immunoreactive LAT1 was detected in the plasma membrane of oocytes injected with wild type 4F2hc and C439S mutant cRNA (Fig. 5B). No immune signal was observed with either wild type LAT1-injected oocytes labeled with pre-immune rabbit IgG

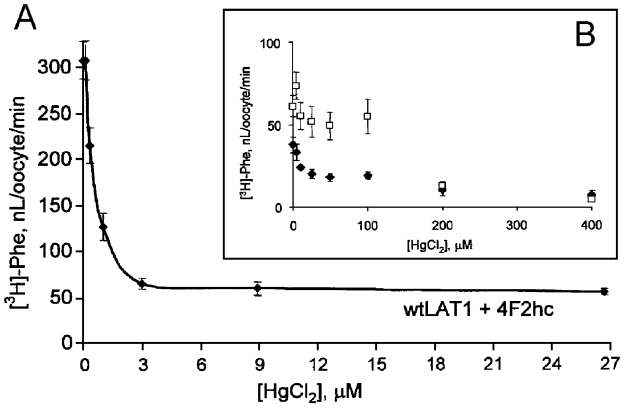

Fig. 3. The clearance (nL/oocyte/min) of [^{3}H]-phenylalanine by frog oocytes was measured in the presence of increasing concentrations of $HgCl_2$. Data are mean±S.E. (n=6 oocytes at each concentration of $HgCl_2$). (A) The oocytes were injected with wild type (wt) rabbit LAT1 and rabbit 4F2hc. (B) The oocytes were injected either with wt rabbit 4F2hc and the C439S LAT1 mRNA (closed squares) or wt rabbit 4F2hc alone (open squares). The uptake of phenylalanine via the endogenous transporter is given in the 4F2hc alone curve.

Table 3
K_i of $HgCl_2$ inhibition of [^{3}H]-phenylalanine transport in frog oocytes injected with rabbit LAT1 cRNA

LAT1 variant	K_i (μM)
Wt	0.56±0.11
C88S	0.54±0.09
C98S	0.72±0.19
C183S	1.44±0.68
C331S	2.90±1.31
C454S	0.80±0.29
C492S	0.72±0.15
C88S/C183S	0.54±0.14
C98S/C183S	1.08±0.35

Mean±S.E., determined by non-linear regression analysis.

(Fig. 5C), or with water injected oocytes labeled with affinity purified anti-LAT1 antibodies (Fig. 5D).

4. Discussion

The high affinity of LAT1 for the LNAAs is a function of the structure of the transporter. The 3-dimensional structure of LAT1 may be similar to that of the bacterial lactose and glycerol-3-phosphate transporters, which are transporters that exhibit a 2-fold symmetry between the amino and carboxyl terminal halves of the protein [9,10]. The predicted structure of the LAT1 transporter is comprised of 12 transmembrane regions [3], and the transporter has 12 phylogenetically conserved cysteine residues [4]. These 12 cysteine residues are nearly symmetrically distributed within the predicted structure of the protein (Fig. 6). There are 5 cysteine residues within transmembrane regions 2–4 and 5 cysteine residues within transmembrane regions 8–12. The Cys^{160} is part of an extracellular loop between transmembrane regions 3 and 4 and forms a disulfide with a cysteine residue of the 4F2hc heavy chain [5]. The twelfth

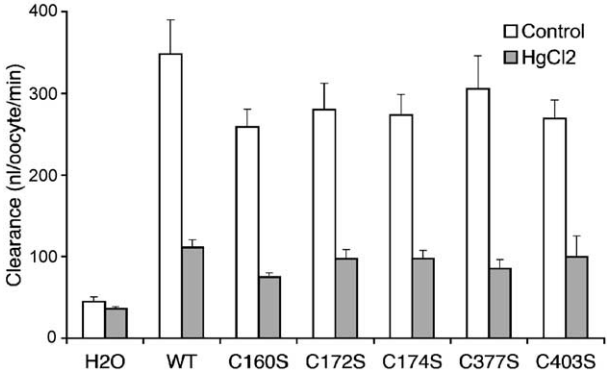

Fig. 4. The clearance (nL/oocyte/min) of [^{3}H]-phenylalanine by frog oocytes was measured in the presence or absence of 2 μM $HgCl_2$. The oocytes were injected with either wild type (wt) rabbit LAT1 and wt rabbit 4F2hc or the indicated mutant of rabbit LAT1 and the wt rabbit 4F2hc. Data are mean±S.E. (n=8–10 oocytes per group). The $HgCl_2$ inhibition of phenylalanine transport via the 5 Cys mutants of LAT1 (C160S, C172S, C174S, C377S, and C403S) was not significantly different from the $HgCl_2$ inhibition of phenylalanine via the LAT1 wild type transporter.

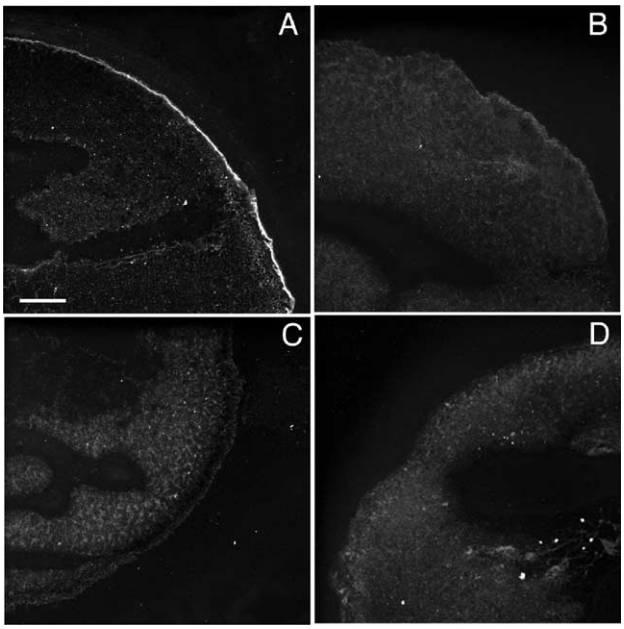

Fig. 5. Confocal microscopy of frog oocytes injected with wild type LAT1 cRNA (A, C), C439S LAT1 mutant (B), or water (D) and labeled with either affinity purified anti-LAT1 antibodies (A, B, D) or pre-immune rabbit IgG (C). Magnification is same in all panels and magnification bar in panel A is 100 μm.

cysteine residue, Cys^{492}, is predicted to lie within the intracellular cytoplasmic tail (Fig. 6). Prior work showed the cloned LAT1 is highly sensitive to inorganic mercury with a K_i of 0.7 μM, but that mutation of Cys^{165} of rat LAT1, which corresponds to Cys^{160} of rabbit LAT1, does not abolish the sensitivity of LAT1 to inorganic mercury [6]. Similarly, mutation of the equivalent Cys^{110} of the rat 4F2hc did not affect the sensitivity of the transporter to inorganic mercury [6]. These results suggested that cysteine residues other than Cys^{160} of LAT1 or Cys^{110} of 4F2hc were responsible for the sensitivity of the LAT1 transporter to $HgCl_2$.

Mutation of either the Cys^{110} or Cys^{332} of rabbit 4F2hc did not inhibit phenylalanine transport (Fig. 1), suggesting that neither of the 4F2hc cysteine residues were important for transporter activity. Mutation of each of the 12 cysteine residues in LAT1 was performed and all 12 mutants were tested for both phenylalanine transport (Fig. 1) and sensitivity to $HgCl_2$ (Table 3, Fig. 4). The $HgCl_2$ K_i for 6 of the mutants was measured and was not different from the wild type transporter (Table 3). The K_i of $HgCl_2$ inhibition of the remaining 5 mutants, at Cys-160, Cys-172, Cys-174, Cys-377, and Cys-403, was not formally determined, because phenylalanine transport via these mutants was not inhibited (Fig. 1), and because the sensitivity of these mutants to $HgCl_2$ was the same as the wild type transporter (Fig. 4). Phenylalanine transport via the C98S, C160S, C172S, C174S, C183S, C331S, C377S, C403S, C454S, and C492S mutants is unchanged (Fig. 1). Phenylalanine transport via the C88S and C439S mutants is impaired, and the

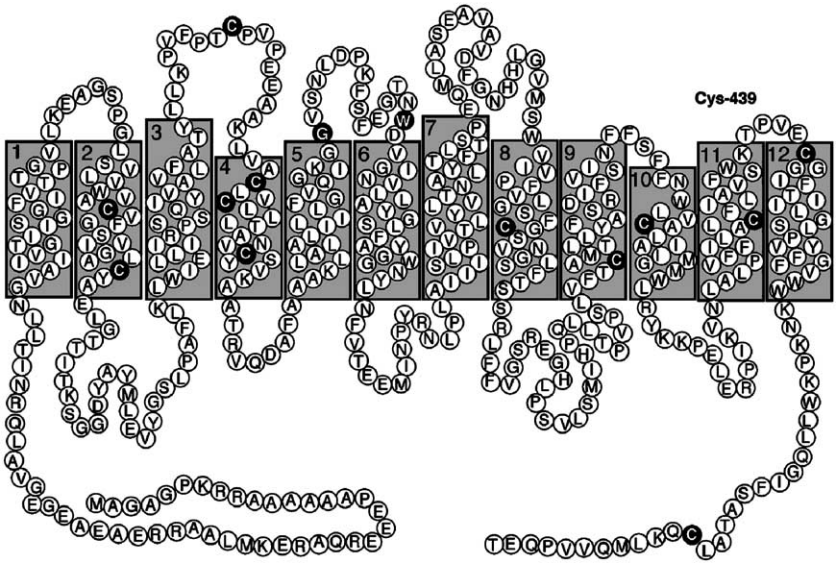

Fig. 6. Twelve trans-membrane region model of rabbit LAT1 shows the position of the 12 cysteine (C) residues. Also highlighted are the Gly^{219} (G) and Trp^{234} (W) residues in the extracellular loop between domains 5–6, as mutation of these residues alters transporter activity [4]. The Cys^{439} residue is predicted to lie within the eleventh trans-membrane region.

V_{max} of phenylalanine transport via the C88S mutant is decreased 50% (Table 2). However, the K_i of $HgCl_2$ inhibition of phenylalanine transport via the C88S mutant, 0.54±0.09 μM, is not different from the $HgCl_2$ K_i of phenylalanine transport via the wild type LAT1, 0.56±0.11 μM (Table 3). The reduction in V_{max} of LAT1 caused by the C88S mutation is eliminated with the double mutant C88S/C183S (Table 2). A similar observation was previously made, wherein the reduced V_{max} caused by the W234L mutation was normalized with the W234L/G219D double mutation [4].

The remaining Cys residue is Cys^{439}, and the rate of phenylalanine transport via the C439S mutant is decreased >90% (Fig. 2). However, the sensitivity of the C439S mutant to $HgCl_2$ could not be assessed because phenylalanine transport into oocytes co-injected with 4F2hc and C439S LAT1 RNA was reduced compared to phenylalanine transport into oocytes injected with 4F2hc alone (Fig. 3B). The C439S mutant light chain may sequester the exogenous 4F2hc, which normally increases amino acid transport via activation of the endogenous oocyte LAT1 homologue [2]. Confocal microscopy showed that the C439S mutant of rabbit LAT1 is not transported to the membrane (Fig. 5). Therefore, among the 12 cysteine residues in LAT1, Cys^{439} plays a unique role in either LAT1 folding or LAT1 insertion in the plasma membrane. It is possible that Cys^{439} is a principal cysteine of LAT1 that is blocked by inorganic mercury. However, this cannot be evaluated because the C439S mutant is not inserted in the oocyte membrane (Fig. 5). Alternatively, inorganic mercury may inhibit LAT1 transporter activity by combining simultaneously with multiple cysteine residues.

In addition to LAT1, other members of this gene family are also sensitive to sulfhydryl reagents, including the human xCT light chain of the cystine/glutamate transporter [11]. The 508 amino acid human LAT1 (accession number AF104032) has a 48% amino acid identity with the 501 amino acid human xCT (accession number AB026891). Both transporters are comprised of 12 trans-membrane domains. The human or rabbit LAT1 has 12 phylogenetically conserved cysteine residues [4], whereas the human xCT transporter has 7 cysteine residues [11], and 4 of these residues overlap with conserved LAT1 cysteine residues, including Cys^{88}, Cys^{160}, Cys^{331}, and Cys^{439} of the rabbit LAT1 (Fig. 6). The cysteine residue of human xCT that is sensitive to membrane impermeant organic mercury reagents is Cys^{327}, which corresponds to Cys^{331} of rabbit LAT1, which is not significantly sensitive to inorganic mercury (Table 3). These comparative findings suggest LAT1 and xCT have different 3-dimensional structures with respect to surface exposed cysteine residues that are reactive with mercuric agents.

The high sensitivity to inorganic mercury of cloned LAT1 expressed in oocytes correlates with earlier in vivo work showing that LNAA transport across the BBB was inhibited by inorganic mercury in blood, and to a greater extent than the mercury-inhibition of other BBB transporters, such as the glucose transporter [12–14]. The inhibition of BBB LAT1 by inorganic mercury may have relevance to the mechanism of neurotoxicity from environmental mercury. The blood concentration of mercury can be as high as 0.08 μM in an adult urban population [15]. Most of blood mercury is likely protein-bound, and may not be accessible to the luminal membrane of the brain capillary endothelium. However, the K_i of $HgCl_2$ inhibition of LAT1 (Table 3) may approximate the plasma level of the metal in acute mercury poisoning. Inorganic mercury is electrically charged and would not be expected to directly cross the

BBB. However, circulating mercury would have access to exposed cysteine residues of BBB transporters expressed at the lumenal membrane of the capillary endothelium. The BBB large neutral amino acid transport is more sensitive to circulating inorganic mercury than is the BBB glucose transporter or the BBB lactate transporter [13]. An inhibition by circulating inorganic mercury of BBB LAT1 would reduce the availability in brain of large neutral amino acids because the rate-limiting step in amino acid transport from blood to brain is the BBB transporter [1]. Inorganic mercury inhibits large neutral amino acid transport with a K_i of 1.8 μM and this is associated with a parallel inhibition of protein synthesis in cultured astrocytes [16]. The rate of amino acid influx into brain across the BBB approximates the rate of amino acid incorporation into brain proteins [1]. Therefore, an inhibition of BBB LAT1 by inorganic mercury in blood could result in impairment of cerebral protein synthesis via an alteration of amino acid availability in brain.

In summary, these studies show that despite the phylogenetic conservation of all 12 cysteine residues of LAT1 (Fig. 6), the individual site-directed mutagenesis of 11 of these cysteine residues does not eliminate the sensitivity of the transporter to inorganic mercury. Mutagenesis of the twelfth cysteine residue, Cys^{439}, produces a transporter that is not inserted in the plasma membrane (Fig. 5B). It is possible that $HgCl_2$ inhibits LAT1 via the concerted inhibition of multiple cysteine residues.

Acknowledgement

This work was supported by National Institutes of Health grant RO1-NS-40016.

References

[1] W.M. Pardridge, W.H. Oldendorf, Transport of metabolic substrates through the blood–brain barrier, J. Neurochem. 28 (1977) 5–12.
[2] R.J. Boado, J.Y. Li, M. Nagaya, C. Zhang, W.M. Pardridge, Selective expression of the large neutral amino acid transporter at the blood–brain barrier, Proc. Natl. Acad. Sci. U. S. A. 96 (1999) 12079–12084.
[3] Y. Kanai, H. Segawa, K. Miyamoto, H. Uchino, E. Takeda, H. Endou, Expression cloning and characterization of a transporter for large neutral amino acids activated by the heavy chain of 4F2 antigen (CD98), J. Biol. Chem. 273 (1998) 23629–23632.
[4] R.J. Boado, J.Y. Li, W.M. Pardridge, Site-directed mutagenesis of rabbit LAT1 at amino acids 219 and 234, J. Neurochem. 84 (2003) 1322–1333.
[5] R. Pfeiffer, B. Spindler, J. Loffing, P.J. Skelly, C.B. Shoemaker, F. Verrey, Functional heterodimeric amino acid transporters lacking cysteine residues involved in disulfide bond, FEBS Lett. 439 (1998) 157–162.
[6] C.A. Wagner, A. Broer, A. Albers, N. Gamper, F. Lang, S. Broer, The heterodimeric amino acid transporter 4F2hc/LAT1 is associated in *Xenopus* oocytes with a non-selective cation channel that is regulated by the serine/threonine kinase sgk-1, J. Physiol. 526 (Pt. 1) (2000) 35–46.
[7] J.Y. Li, R.J. Boado, W.M. Pardridge, Differential kinetics of transport of 2′,3′-dideoxyinosine and adenosine via concentrative Na+ nucleoside transporter CNT2 cloned from rat blood–brain barrier, J. Pharmacol. Exp. Ther. 299 (2001) 735–740.
[8] J.Y. Li, R.J. Boado, W.M. Pardridge, Cloned blood–brain barrier adenosine transporter is identical to the rat concentrative Na+ nucleoside cotransporter CNT2, J. Cereb. Blood Flow Metab. 21 (2001) 929–936.
[9] J. Abramson, I. Smirnova, V. Kasho, G. Verner, H.R. Kaback, S. Iwata, Structure and mechanism of the lactose permease of *Escherichia coli*, Science 301 (2003) 610–615.
[10] Y. Huang, M.J. Lemieux, J. Song, M. Auer, D.N. Wang, Structure and mechanism of the glycerol-3-phosphate transporter from *Escherichia coli*, Science 301 (2003) 616–620.
[11] M. Jimenez-Vidal, E. Gasol, A. Zorzano, V. Nunes, M. Palacin, J. Chillaron, Thiol modification of cysteine 327 in the eighth transmembrane domain of the light subunit of xCT of the heteromeric cystine/glutamate antiporter suggests close proximity to the substrate binding site/permeation pathway, J. Biol. Chem. 279 (2004) 11214–11221.
[12] O. Steinwall, Brain uptake of Se75-selenomethionine after damage to blood–brain barrier by mercuric ions, Acta Neurol. Scand. 45 (1969) 362–368.
[13] W.M. Pardridge, Inorganic mercury: selective effects on blood–brain barrier transport systems, J. Neurochem. 27 (1976) 333–335.
[14] H. Hervonen, O. Steinwall, Endothelial surface sulfhydryl-groups in blood–brain barrier transport of nutrients, Acta Physiol. Scand. 121 (1984) 343–351.
[15] M. Weil, J. Bressler, P. Parsons, K. Bolla, T. Glass, B. Schwartz, Blood mercury levels and neurobehavioral function, JAMA 293 (2005) 1875–1882.
[16] N. Brookes, D.A. Kristt, Inhibition of amino acid transport and protein synthesis by $HgCl_2$ and methylmercury in astrocytes: selectivity and reversibility, J. Neurochem. 53 (1989) 1228–1237.